Net Carbon Dioxide Emission from An Eroding Atlantic Blanket Bog

Rebekka Artz (rebekka.artz@hutton.ac.uk)
The James Hutton Institute Aberdeen https://orcid.org/0000-0002-8462-6558
Mhairi Coyle
The James Hutton Institute
Gillian Donaldson-Selby
The James Hutton Institute
Ross Morrison
UK Centre for Ecology & Hydrology

Research Article

Keywords: Peatland, blanket bog, peat erosion, carbon dioxide, net ecosystem exchange, 22 restoration, eddy covariance

Posted Date: November 11th, 2021

DOI: https://doi.org/10.21203/rs.3.rs-991712/v1

Version of Record: A version of this preprint was published at Biogeochemistry on April 20th, 2022. See the published version at https://doi.org/10.1007/s10533-022-00923-x.

Net carbon dioxide emissions from an eroding Atlantic blanket bog

Rebekka R.E. Artz[1*], Mhairi Coyle[1,2], Gillian-Donaldson-Selby[1], Ross Morrison[3]

[1] The James Hutton Institute, Craigiebuckler, Aberdeen, AB15 8QH, UK

[2] UK Centre for Ecology & Hydrology, Bush Estate, Penicuik, Midlothian, EH26 0QB, UK

[3] UK Centre for Ecology & Hydrology, Maclean Building, Benson Lane, Crowmarsh Gifford, Wallingford, Oxfordshire, OX10 8BB, UK

*Corresponding author: rebekka.artz@hutton.ac.uk; https://orcid.org/0000-0002-8462-6558

Abstract

The net impact of greenhouse gas emissions from degraded peatland environments on national Inventories and subsequent mitigation of such emissions has only been seriously considered within the last decade. Data on greenhouse gas emissions from special cases of peatland degradation, such as eroding peatlands, are particularly scarce. Here, we report the first eddy covariance-based monitoring of carbon dioxide (CO_2) emissions from an eroding Atlantic blanket bog. The CO_2 budget across the period July 2018 to November 2019 was 147 (+/- 9) g C m^{-2}. For an annual budget that contained proportionally more of the extreme 2018 drought and heat wave, cumulative CO_2 emissions were nearly double (191 g C m^{-2}) of that of an annual period without drought (106 g C m^{-2}), suggesting that direct CO_2 emissions from eroded peatlands are at risk of increasing with projected changes in temperatures and precipitation due to global climate change. The results of this study are consistent with chamber-based and modelling studies that suggest degraded blanket bogs to be a net source of CO_2 to the atmosphere, and provide baseline data against which to assess future peatland restoration efforts in this region.

Keywords Peatland, blanket bog, peat erosion, carbon dioxide, net ecosystem exchange, restoration, eddy covariance

Declaration RA and RM were responsible for experiment design, GDS and MC caried out site maintenance, RA, MC and RM shared data processing and analysis elements, RA led the writing of this manuscript, with contributions from all co-authors. RA, GDS and MC were part supported for this project by the Rural & Environment Science and Analytical Division of the Scottish Government (Strategic Research Programme 2016-2021), with RA providing additional, unfunded, time. RM was supported by the Natural Environment Research Council award number NE/R016429/1 as part of the UK-SCAPE programme delivering National Capability. We gratefully acknowledge NatureScot Peatland Action funding for the initial acquisition of the eddy covariance equipment. The annual

budget of a shorter, daily, timeseries of this site was used in a recent synthesis publication (Evans et al., 2021). The 30-minute processed data for this manuscript are available from the UK Environmental Information Data Centre (EIDC), with the identifier: https://doi.org/10.5285/a65f6241-bfc3-430a-ae93-ccb7c63c1a53. There are no competing interests to declare. None of the authors received direct remuneration for any advisory roles undertaken or had any financial or non-financial interests in organisations that may be affected by the results of this study.

Introduction

Peatlands are the world's most effective terrestrial carbon store, with around 500 Gt (15 to 30% of the world's soil carbon) stored, despite such ecosystems only occupying around 3% of the terrestrial land area (Limpens et al. 2008; Yu et al. 2012). Peatlands in their intact states that are still located within suitable bioclimatic envelopes accumulate and store carbon because photosynthetic uptake of C exceeds the losses via respiration and anaerobic decomposition (e.g., Waddington et al. 2015). Degradation by direct human disturbance, such as drainage, grazing and land use conversion, as well as the influence of climate change, can switch peatlands from net sink to net sources of C. Globally, peatlands turned from a net carbon sink to a net source around the 1960s, due to extensive drainage and land use conversion, particularly in Europe and South-East Asia (Leifeld et al. 2019). Expert assessments compiled by Loisel et al (2021) assert that the combined effects of land use and climate change-driven changes in global temperature, precipitation patterns and fire risk will result in even stronger impacts on peatland carbon stocks in the near (to 2100) and far (2100-2300) future. Cumulative emissions from drained peatlands are estimated to have reached 80 ± 20 Pg CO_2e in 2015, with further increases due to continued drainage of peatlands in many areas of the world. This may lead to total peatland emissions of up to 249 ± 38 Pg by 2100 (Leifeld et al. 2019). Moreover, global warming is likely to reach 1.5°C between 2030 and 2052 if it continues to increase at the current rate (IPCC, 2018) which, together with projected changes to precipitation patterns (e.g., Giorgi et al., 2019), make the fate of this vast global peatland C stock highly uncertain.

Peatland restoration has been recognised as a cost-effective way to mitigate CO_2 emissions alongside improving the intrinsic value of these threatened habitats (Paustian et al. 2016). Leifeld and Menichetti (2018) used the 2013 IPCC Wetland Supplement default (Tier 1) emission factors combined with a bespoke global mapping effort of the various IPCC land use categories on peat soils

to arrive at an estimate of 0.31–3.38 Gt CO_2-equivalent of emissions per annum from the world's peatlands, with much of it stemming from CO_2. Clearly, there is further refinement of this estimate required, and particularly high uncertainties in the emission factors are in the less intensively managed peatland categories. Peat erosion, in particular, is difficult to allocate to a specific IPCC land use category and furthermore is often excluded from broad land cover mapping efforts. Peat erosion occurs around the world (e.g., Yunker et al. 1991; Wilson et al. 1993; Pastukhov and Kaverin 2016; Selkirk and Saffigna 2018), although the literature on erosion rates and resulting C losses is heavily dominated by studies from the UK and Ireland (e.g., Bradshaw and McGee 1988; Birnie 1993; Carlin et al. 1997; Bragg and Tallis 2001; Evans and Warburton 2007; Tomlinson 2009).

Peat erosion not only contributes to direct losses of carbon; erosion gullies divert water and thus constitute a form of drainage that may affect plant photosynthetic responses and soil respiration. While direct C losses from eroding peatlands through particulate and dissolved organic carbon in fluvial and windborne erosion paths have understandably received much scientific attention, less is known about the direct gaseous emissions from these carbon dense ecosystems. Existing data on GHG emissions from eroded peatlands stem entirely from chamber-based studies (McNamara et al. 2008; Clay et al. 2011; Worrall et al. 2011; Gatis et al. 2019), which require careful inclusion of the many different components of erosion features in the landscape and upscaling. Without robust understanding of the current emissions from eroded peatland ecosystems, the cost effectiveness of restoration work through gully blocking, reprofiling and re-vegetation of bare areas cannot be determined, and neither can overall GHG abatement potential be estimated from such activities. Data on the overall area of eroded peatlands in UK blanket bogs is also still scarce and many estimates do not break down the figures into the area directly affected by erosion (i.e., bare) versus the wider area that is indirectly affected due to the altered surface hydrology.

Here, for the first time, CO_2 fluxes measured using the eddy covariance (EC) technique are presented for an eroding oceanic blanket bog located in the Cairngorms, Scotland. Our objectives for this study were to: 1) quantify the magnitude of the net ecosystem exchange (NEE) of carbon dioxide (CO_2); 2) explore effects of short-term variation in local climate on CO_2 fluxes; and 3) set the quantitative baseline against which the abatement potential of future restoration management can be evaluated.

Methods

Site location, description, and climate

97 The study took place on a large high-altitude plateau blanket bog in the eastern part of the
98 Cairngorms National Park, Scotland, UK (56.93° N, -3.16° E, 642 m asl). The climate at the site is
99 maritime temperate montane and is located on the edge of Köppen-Geiger class Dfc (cold, no dry
100 season, cold summer, as per Beck et al. 2018). The nearest long-term UK Met Office station is
101 Braemar (57.006 N, -3.396 E, 327 m amsl) which has a mean annual (1981 to 2010) maximum and
102 minimum air temperature and precipitation of 10.7°C, 3°C and 932 mm yr^{-1}, respectively. The wider
103 Cairngorms area experiences significant snowfall, and between 30 to more than 60 snow days each
104 year, although a significant decline in snow days and snow depth has been observed over recent
105 decades (Rivington & Spencer, 2020), especially at higher altitudes. Snowfall in the region in recent
106 years has been generally sporadic, rather than providing a single snow-covered period. It is not
107 possible to provide estimates at the site prior to the monitoring period, but they are likely to fall on
108 the lower end of the range. Peat erosion is widespread (Fig. 1) and bare peat gullies vary between
109 0.5 – 3 m in their depth and 2->10 m in their width. The surface area occupied by bare peat in
110 erosion features was mapped using high resolution aerial photography (25 cm resolution,
111 GetMapping) dated 2019 and further by high resolution LiDAR (12 cm horizontal, 3 cm vertical) in
112 November 2020. Ground control locations of vegetated and bare peat areas exceeding a minimum
113 area of 5 m^2 were collected with a handheld GPS (Garmin Etrex, locational accuracy 3 m). Supervised
114 classification analysis, using the ground control point locations, was carried out using the semi-
115 automated classification plug-in (Congedo, 2016) in QGIS version 2.18.4.

116 Peat depth ranges from <0.2 m to > 2m across a neighbouring area in the catchment similar
117 in slope and aspect to the flux tower footprint, based on a 100 m grid-based survey (Peatland Action
118 data, S. Corcoran, Cairngorms National Park Authority, *pers. Comm*.) which sampled gullies as well as
119 vegetated peat. It is not possible to estimate average peat depth in the gullies versus vegetated
120 areas from these data as the data did not include attributes to differentiate these terrain types and
121 the positional accuracy of the GPS used is insufficient to assess this through overlays with aerial
122 photography. The peat depths in the wider catchment area are largely similar, with a few notably
123 deeper points of up to 6 m. The peat pH was between 3.1-3.4. Water levels were unknown prior to
124 this study. Vegetation composition is typical of eastern Scotland elevated blanket bog [largely M19
125 *Calluna vulgaris* – *Eriophorum vaginatum* blanket mire], with a mean canopy height of 0.25 m. The
126 wider landscape is predominantly managed for red deer (*Cervus elaphus*) and red grouse (*Lagopus*
127 *lagopus*), with some managed burning (muirburn) applied occasionally, though none within the 2
128 km^2 area surrounding the site within the monitoring period reported on in this work. Other grazing
129 animals are mountain hare (*Lepus timidus*) and occasional roe deer (*Capreolus capreolus*).

130 Eddy covariance measurements

Sensible and latent heat fluxes (LE and H, respectively) and NEE were monitored using an enclosed path EC system. The EC system combined a Windmaster (Gill Instruments Ltd. Lymington, UK) sonic anemometer at 3.2 m above the peatland surface for the components of atmospheric turbulence (u, v, w; m/s) and sonic temperature (Tsonic; °C), with an LI-7200 enclosed path H_2O/CO_2 gas analyser (Li—COR Biosciences, Lincoln, Nebraska, USA L) to measure atmospheric mass density of vapor (g H_2O/m^3) and CO_2 (mg CO_2/m^3) as well as barometric pressure (Pair; kPa). The horizontal separation between the sonic anemometer and the Li-7200 was 0.1 m. The length of LI-7200 inlet tube was 1.0 m, optimised for measurements of CO_2 mass density over H_2O (e.g., LI-7200 RS instruction manual, Li-COR, 2015). Air temperature (Ta; °C) and relative humidity (RH; %) were measured at 2 m above the peatland surface using a Rotronic Hygroclip (HC2-S3, Rotronics, Darlaston, Wednesbury, UK). EC sensors were sampled and logged at 20 Hz using a CR3000 Micrologger (Campbell Scientific Inc., Logan Utah). The system was installed on a fully vegetated piece of land as the surfaces of the bare peat gullies tend to move during the winter months due to frost heaving. The available fetch in the prevailing wind direction (SW) was >1000 m, in all wind directions except N where a cliff edge limits the fetch to ca. 400 m. Canopy height (0.25 m) was assumed to be static throughout the year; the vegetation is semi-evergreen with light to locally moderate deer grazing pressure.

A range of micrometeorological measurements were carried out on the same mast as the EC data collection. Net radiation (Rnet; W m^{-2}) and its incoming and outgoing short- and long-wave components (SWin, SWout, LWin, and LWout, respectively; W m^{-2}) were measured above the canopy (2.06 m above the peatland surface) using an SN500 Net Radiometer (Apogee Instruments Inc. Logan, Utah, USA). PAR was measured at 2.25 m using a SKP215 Quantum Sensor (Skye Instruments, UK). Soil physics were measured close to the EC mast (within a radius of 5 m). Soil heat fluxes (G; W/m^2) were monitored using two HFP01SC soil heat flux (Hukseflux BV, BV, Delft, The Netherlands) plates installed at 0.03 m below the surface. Soil temperature (Tsoil; °C) was measured at a depth of 2, 5, 10, 20 and 50 cm below the peatland surface using an STP01 soil temperature profile (Campbell Scientific Inc., Logan, Utah, USA). Soil volumetric water content (VWC; m^2) and additional soil temperature measurements were made using four Digital Time Domain Transmissometry (TDT) probes (TDT Soil Water Content sensor, Acclima, Idaho, USA) installed vertically at 5, 10, 15 and 20 cm depth. Precipitation was measured using a SBS500 unheated tipping bucket rain gauge (P; 0.2 mm sensitivity; Environmental Measurements Ltd, Newcastle, UK) installed in an open area free of any obstruction. Water table depth was measured using a CS451 pressure sensor (Campbell Scientific Inc., Logan, Utah, USA) installed in a 32 mm diameter PVC well with alternating 3 mm holes at 50 mm distance on 4 rows along the profile). The aforementioned sensors

were scanned at 0.1 Hz and logged as 30-minute means (sums for precipitation). An additional 3 were installed on vegetated ground within 20 m of the mast (1 m capacitance water level loggers, Odyssey, New Zealand) starting autumn 2019, and a further 4 standalone water level loggers were installed in dipwells approximately 1 m away from gully edges next to two pairs of gullies in the wider eroded catchment in spring 2020.

EC data handling

Thirty-minute flux densities (hereafter fluxes) of sensible and latent heat (LE and H) and net ecosystem CO_2 exchange (NEE) were computed from the raw EC data using EddyPRO® Flux Calculation Software (v 7.0.6; LI-COR Biosciences, Lincoln, Nebraska; Fratini & Mauder 2014). Raw EC data were screened for statistical outliers (Mauder et al. 2013) and other physically implausible values (Vickers & Mahrt 1997). Sonic anemometer data were rotated using a two-dimensional coordinate rotation procedure (Wilczak et al. 2001) and corrected for imperfect cosine response (Nakai et al. 2012). A planar rotation was also tested but did not provide significant improvements. No boost bug correction was required for the Windmaster deployed at the site (firmware version 2329.700.01). Time lags between the vertical wind speed and concentration measurements were removed using a cross-correlation procedure. Uncorrected fluxes were calculated as the mean covariance between the vertical wind speed (w) and the respective atmospheric scalar using 30-minute block averages (Baldocchi 2003). Fluxes were corrected for high (Moncrieff et al. 1997) and low frequency cospectral attenuation (Moncrieff et al. 2004). H fluxes were corrected for the influence of atmospheric humidity (Schotanus et al. 1983). LE, then CO_2, fluxes were adjusted for fluctuations in atmospheric density (Webb et al. 1980). Random uncertainties for 30-minute flux observations related to sampling error were estimated as standard deviations derived from a variance of covariance approach (Finkelstein & Sims 2001). CO_2 storage was assumed negligible at the low observation height and NEE was assumed equal to the turbulent CO_2 flux. The micrometeorological sign convention is adopted where positive values represent fluxes from ecosystem to atmosphere and negatives describe the opposite state.

Quality control (QC) procedures were applied to ensure only high-quality turbulent flux data were retained for analysis. Thirty-minute flux data were screened for statistical outliers using the median absolute deviation approach (Sachs, 2013) following recommendations in Papale et al. (2006). Fluxes were also excluded when: the results of the stationarity (steady-state) test result deviated by more than 100% (Foken et al. 2004); and when fluxes were outside the range $-200 < H > 450 W/m^2$, $-50 < NEE > 30$ µmol CO_2 m^2, and $-50 < LE > 300$ W/m^2. Periods of low turbulent mixing were identified using a friction velocity (u*) threshold approach (Papale et al. 2006; Reichstein et al.

2016), and CO_2 fluxes were excluded when u* < 0.17 m/s. A 2D footprint model was also calculated as per Kljun et al (2015). Overall energy balance closure (EBC; SI Fig. 1) for the system was 0.8, which is within the range attained for EC sites globally (Leuning et al. 2012; Stoy et al. 2013; Wilson et al. 2002), and acknowledging that the length of the inlet tube of the Li-7200 was optimised for CO_2 flux measurements.

Gap-filling of flux data and the partitioning of NEE into estimates of gross ecosystem production (GEP) and total ecosystem respiration were performed using the REddyProc Package version 0.8-2/r14 (Reichstein et al. 2016) for the R statistical Language (R Core Team, 2017). Data gap-filling of H, LE, and NEE was performed using the marginal distribution sampling (MDS) approach (Reichstein et al. 2005). To enable annual sums to be computed, gaps in air temperature were gap-filled using interpolation of observations from the Braemar station (57.011, -3.396, 327m asl). Details of the MDS and flux partitioning algorithms have been described in detail and evaluated elsewhere (Desai et al. 2008; Moffat et al. 2007; Papale et al. 2006; Reichstein et al. 2005) and are not repeated here. Standard night-time-based flux partitioning was used, although we note that this approach has been questioned recently for peatland ecosystems by Järveola et al. (2020). Gaps in prognostic micrometeorological variables (SWin, Tair) required for MDS gap-filling were filled using observations obtained at Braemar. Tair was used as the driving temperature for flux partitioning as a number of data gaps were present in the Tsoil record. Uncertainty for individual gap-filled fluxes was estimated as the standard deviation of the observations averaged to fill data gaps (Reichstein et al., 2016). No uncertainties were estimated for GEP and TER as the partitioned CO_2 fluxes represent modelled quantities. During the time period of monitoring, no wildfires occurred, and as grazing pressure could not be determined, we assume that NEE equals NEP.

Light and night-time respiration response analyses

NEE during the growing season (April to October) was used to parameterise a modified Michaelis-Menten equation as a function of incoming short-wave radiation (SW*in*), using:

$$NEE(SWin) = \frac{-\propto SWin}{1 - (SWin/900) + (\propto SWin/900)} + Rm$$

Where α (µmol CO_2 J^{-1}) is the ecosystem quantum yield, GPP_{900} (µmol CO_2 m^{-2} s^{-1}) is the rate of photosynthesis when SW*in* is 900 W/m^2 and R*m* (µmol CO_2 m^{-2} s^{-1}) is the mean ecosystem respiration rate (Carrara et al. 2003; Falge et al. 2001). We also fitted an exponential temperature response model (Lloyd and Taylor, 1994) using the night-time NEE (assumed to be equivalent to ecosystem respiration), and evaluated the residuals against water table depth as per the expectation

that the site would conform to findings of others that peatland nocturnal respiration is driven primarily by temperature and water table (e.g., Laine et al. 2005).

Results

Spatial representativeness

The flux footprint (predominantly into the South-westerly direction) included the area affected by erosion at all times (Fig. 1), but spring observations in particular included less of the eroded area and more of the fully vegetated surface closest to the tower location. The classification analysis of the wider unrestored area surrounding the flux tower footprint returned proportions of 83.9% vegetated ground, 15.3% bare peat in erosion gullies (in 2 dimensions, i.e., not taking into account gully sides) and 0.8% standing water bodies. The footprint captured a representative area of the wider eroded catchment. Mean x peak and 90% of the footprint were 46.7 and 128.1 m at night, and 46.2 and 126.5 m during daytime, respectively. The maximum 90% of the x footprint was 1414 m at night and 770 m during daytime.

Environmental conditions

Environmental conditions at the Balmoral station are shown in Fig 2. Based on long-term observations from the nearby Braemar weather station (SI Fig 2), 2018 was ranked 22nd for total annual precipitation out of 60 years of observation (1961-2020), and also followed the fifth driest year (2017) within that record. Relative to the most recent 30-year average period (1981-2010), 2018 was characterised by much lower-than-average precipitation for the first half of the year but heavy rainfall during November (SI Fig. 2). 2018 had a relatively cool start to the year, followed by an abrupt change to an extreme heat wave for the months May to July, peaking at 3.7 °C above the 1981-2010 maximum temperature during June. This was followed by relatively average temperatures during the autumn period and a slightly warmer than average winter 2018-19. In the biomet data series from our higher altitude site, these unusual conditions were reflected in the water table dynamics, which displayed a much lower water table depth between July and November 2018 than in the other two years (Fig. 2). The year 2019, in contrast, was at the wetter end of the range, occupying rank 49 out of 60 years of observation (1961-2020) for Braemar, with 6 months of higher-than-average precipitation, mostly during the first half of the year. The only deviations in minimum or maximum air temperature occurred during the winter periods. In the data from our monitoring site, this is evident in a period of high air and soil temperatures in February 2019 compared with the other two years of observations. We observed only a brief period of water table

drawdown during late April 2019 (Fig. 2). 2020 was another year with higher-than-average spring and summer air temperatures at Braemar, as well as a milder than average early winter. Precipitation records at Braemar also show a sustained drought between March and June 2020, followed by higher-than-average summer rainfall and another short drought in September (SI Fig. 2). At our higher altitude site, water table depth records suggest significant drought between April and September 2020 and some short periods of higher-than-average air and soil temperatures in the same timeframe, compared with the other years of observation (Fig. 2).

Data capture

Data capture over the monitoring period up to 14th of November 2019 resulted in 91% coverage in flux observations. Biomet data capture was between 92-97% except for long wave radiation (79%) due to a faulty sensor, and snow depth (88%, Fig. 2). All data between the 14th of November to the 27th of December 2019 were unfortunately lost due to a major power supply issue. During the same time, peatland restoration activities were carried out in nearby areas, which produced wind-blown peat particles that entered the gas analyser, and which severely affected the spectral response seen in data from the Li-7200RS. Due to COVID travel restrictions at this time, it was not possible to fix this issue until August 2020 and hence NEE and LE data until mid-August 2020 had to be discarded. Biomet data capture continued during this time and was 88-91% except for shortwave (88%) and longwave (76%) radiation components. Remaining observations for the period July 2018 until November 2020 following QC were 35% (CO_2), 19% (LE), 61% (H), 80% (Rg), 87% (Tair), 87% (Tsoil) and 82% (VPD), Fig 2.

Seasonal/diurnal patterns and light/night-time temperature response of CO_2 fluxes

In general, net ecosystem exchange of CO_2 (NEE) was positive, except for daytime periods between May and October (SI Fig 3). The range of NEE was -14.06 to 13.90 µmol m^{-2} s^{-1}, with maximum net uptake from the atmosphere during daylight hours in the months of July and August and maximum emissions to the atmosphere during nocturnal periods during autumn, early winter and early spring. The 2018 drought resulted in a slight decrease in net uptake during daylight hours and slightly higher nocturnal net emissions compared with the other two years of observations. Due to the altitude of the site and hence frequent cloud cover, maximum modelled partitioned GEP varied significantly between years, with maxima occurring between July and September (Fig 3). Occasional spikes in emissions were observed in winter periods, corresponding to periods following partial or complete snow cover within the footprint. Modelled R_{eco} was noticeable higher during 2018 than 2019, as was GPP during the main growing season (Fig 3). 2018 was a drought year, with nearly twice as much precipitation during the autumn of 2019 compared with 2018, after an early summer period of

warmer than normal air temperatures in 2018 (Fig 3). These circumstances resulted in a significantly lower summer water table in 2018 than in 2019 and 2020, lasting into the next year (Fig 2, plotted as annual values in SI Fig. 3).

Modelled parameters for the NEE light response over the summer periods within the 18 months of data capture (Table 1) were roughly in line with other published parameters for peatland ecosystems with semi-natural vegetation cover (e.g., Pelletier et al. 2015). Due to the relatively uniform distribution of the gullies amongst the landscape within the footprint (Fig 1) we were unable to build separate models for partial footprints that may have contained differential proportions of eroded surface area. Mean GPP_{max} over summer periods within the 28-month monitoring period was 7.65 µmol m^{-2} s^{-1}, α was 0.031 µmol CO_2 J^{-1}, and the mean respiration rate Rm was 1.68 µmol CO_2 m^{-2} s^{-1}. Monthly values are given in Table 1.

The temperature response of nocturnal NEE showed only a very weak correlation with air or soil temperature, and similarly, very weak correlation of the residuals of the temperature-NEE response when analysed against water table depth dynamics (not shown). We attempted further data analysis by omitting periods with and immediately after snow fall or extreme cold snap periods (which are highly episodic in nature and often interspersed with periods of milder weather, and in some years occurring as late as mid-May). Snow of any significant depth tends to only accumulate in the gullies, which are also prone to significant frost heave. Omitting periods with or subsequent to snowfall did not improve temperature response fits. We also tried omitting data from nights with fewer than 7 available half-hours of night-time NEE (e.g., Helbig et al., 2019), as well as choosing soil temperature instead of air temperature, however neither of these improved the model fit.

Net ecosystem carbon dioxide balance

Overall, periods of net CO_2 uptake from the atmosphere were limited to summer periods between late June and late August (Fig 3), and even during this time, daily fluxes were frequently small net emissions to the atmosphere. Overall, the site was a net source of carbon dioxide of 147 g (+/- 9) CO_2-C m^{-2} during the 18-month period of July 2018 to November 2019 (Fig. 3). Annual C balances calculated using a moving window for all 365 days intervals within this period ranged between 106 and 191 g CO_2-C m^{-2} y^{-1}. Higher annual C balances were obtained in cumulative 365-day budgets that included the end of the summer 2018 drought, while during 365-day periods with starting dates closer to November 2018, the site was a lower net source of CO_2. Finally, we assumed that any additional biomass offtake term through grazing would be negligible, due to the low density of grazing animals and lack of significant browsing damage, however we do not have data to allow us to verify this.

Discussion

This is the first report of carbon dioxide (CO_2) fluxes, measured using the eddy covariance technique, in an eroded mountain peatland ecosystem. The magnitude of instantaneous CO_2 fluxes and the light use response at this eroded blanket bog is within the range of previously reported figures for degraded peatlands in the temperate zone (e.g., Lafleur et al., 2003). Specific observations of CO_2 fluxes from eroded peatlands are very sparse, based on chamber measurements, and either report only summer fluxes or suffer from significant data gaps over winter months due to the challenges of accessing mountain environments and carrying out manual measurements of carbon dioxide flux during snow cover. Gatis et al (2019) estimated, using an empirically derived net ecosystem model estimated that, over two growing seasons (May to September at their site location at considerably lower altitude and latitude), both vegetated hags (29 and 20 g C m^{-2}; 95% confidence intervals of -570 to 762 and - 873 to 1105 g C m^{-2}) and the eroded peat pans (7 and 8 g C m^{-2}, 95% confidence intervals of – 147 to 465 and - 136 to 436 g C m^{-2}) were net carbon sources.

Dixon et al (2014) and Clay et al (2012) do not report an annual budget for their study sites on an eroded plateau blanket bog (lower altitude and latitude than the present study) comprising both bare and revegetated (following restoration activities) gullies, but observe that the two bare gullies included in the design were net CO_2 sources on average over a 5-year monthly chamber-based monitoring campaign (24 and 32 mg CO_2 m^{-2} h^{-1}, respectively). Their studies included winter fluxes, but typically only managed to capture ~25% of winter monitoring campaigns due to snow or equipment failures.

Similarly, data from vegetated parts of high-altitude blanket bog are limited to a small number of studies. Clay et al (2010) report 156 g C m^{-2} y^{-1} of carbon dioxide emissions from a site in the north of England, again at lower latitude and altitude than the present work and using chamber-based approaches. Dixon et al (2015) further reported upland blanket bog sites with predominant cover of heather (*Calluna vulgaris*), as in the case of the present study and in degraded temperate oceanic blanket bog more generally, to be a net CO_2 source, with an increase in flux for increased canopy height. Using high resolution digital surface mapping rather than GHG flux monitoring, Evans and Lindsay (2010) reported an upland blanket bog to be a current net carbon source of 29.4 g C m^{-2} y^{-1}. Our study represents the first publication of carbon dioxide emissions from eroded peatland that includes all of the landscape elements and winter fluxes, and suggests that net losses are generally higher than in previous, chamber-based or mapping-based, reports.

Overall, the reported CO_2 fluxes from this eroded blanket bog fall into the lower end of the same range as reported for the IPCC Wetland Supplement for temperate peat extraction sites, i.e., sites

where all vegetation has been removed: the Tier 1 emission factor is 280 (110–420) g C m^{-2} y^{-1} (95% CI in brackets, IPCC, 2014). Wilson et al (2015) subsequently reported lower Tier 2 emission factors of 170 (+/- 47) g C m^{-2} y^{-1} for industrially extracted, entirely bare, sites and 164 (+/- 44) g C m^{-2} y^{-1} for domestic peat extraction sites. The high emissions from this site, where only ~15% of the surface was occupied by bare peat, are therefore concerning. The approach taken for inclusion of peatland emissions in UK Inventory reporting (Evans et al. 2017), due to the paucity of data from eroded peatland at the time, was to produce a weighted average emission factor for eroded peatlands, comprising calculated Tier 2 emission factors for slightly modified, semi-natural peatland and extracted, bare, peat surfaces. This approach resulted in much lower estimated CO_2 emissions for eroded peatland (20 g C m^{-2} with a 95% confidence interval of -10 to 60) than the results of this study suggest. It is therefore likely that emissions from eroded peatlands in the UK are underestimated in the current UK Emissions Inventory submission.

In contrast, carbon dioxide fluxes from hydrologically intact or near-intact peatlands are generally reported to be strongly net negative to the atmosphere, i.e., carbon sinks (for blanket bog e.g., Levy and Gray, 2015; Helfter et al., 2015, Sottocornola and Kiely, 2010, 2005). Our findings therefore support an argument for restoration of this eroded site. The most convincing example of the benefits of rewetting to date stems from Canadian peatland studies of long-term experiments by Nugent et al., 2019, Lee et al. (2017) and Strack and Zuback (2013). In a blanket bog context, Hambley et al (2019) show net CO_2 flux, monitored by eddy covariance, from former forestry-converted sites returning to similar values to that of a nearby undisturbed low altitude blanket bog. Wilson et al. (2016) and Renou-Wilson (2019) similarly show significant mitigation of carbon dioxide emissions following rewetting of former peat extraction sites.

In a recent synthesis of GHG fluxes from peatlands, and to which this work contributed with a shorter time series of the data presented here, Evans et al (2021) concluded that water table depth was the highest explanatory factor of net ecosystem exchange of carbon dioxide over the medium term and thus peatland rewetting could contribute significantly to efforts to reduce emissions from degraded peatlands. Water table depth monitoring at the Balmoral site only began in early August 2018 and hence we can only calculate the corresponding NEE for the moving window period from this point onwards. For the first 365-day window (4th August 2018-2019), the annual loss of CO_2 was 175 g C m^{-2} at a mean annual water table depth of -10.15 cm. For the latest possible 365-day window (14th November 2018 – 2019), the site lost 106 g C m^{-2} of CO_2 at a corresponding mean annual water table depth of -8.97 cm. However, as water table depth monitoring in this phase was only carried out in the direct vicinity of the instrumentation, it is likely that the mean annual water table depths are not applicable to the wider footprint. Indeed, additional monitoring results within

the wider footprint, once the full complement of loggers was installed in spring 2020, show that there was a significant water level drawdown on vegetated areas adjacent to bare peat gullies during summer months (Fig 4). The true annual mean water table depth is therefore likely to be significantly lower. Additional measurements will be required to shed further light on the likely true water table dynamics at this site, potentially in conjunction with footprint-wide hindcasting into the monitoring period reported on in this work, using modelled water table dynamics from the reported relationship between peatland water table dynamics with synthetic aperture radar C-band backscatter (e.g., Bechtold et al. 2018; Lees et al. 2021). Finally, although no prescribed burning or wildfires occurred within the footprint during the years of monitoring, however, for a complete C budget, we would also require information on the net methane fluxes to or from the atmosphere and any net losses via aquatic routes. The latter are likely to be substantial as there is evidence of ongoing erosion after rainfall events, but data on this are not available at present.

Some atypical observations in our study system do warrant discussion and further evaluation. In contrast to published observations of relationships of night-time NEE with temperature in natural, degraded and rewetted peatlands (e.g., Herbst et al, 2013, Laine et al., 2005; Helbig et al., 2019, Lee et al., 2015), we were unable to find a satisfactory fit to an exponential Lloyd-Taylor model, using either air or soil temperature, nor by omitting periods during or immediately following snowfall or potential frost-heave, or by omitting nights with fewer than 7 observations. We hypothesize that the most likely cause of these observations is sensor mismatch of the air/soil temperature probes and the pressure transducer (for water table depth) relative to the wider footprint, as these are placed in the area immediately surrounding the installation, which is fully vegetated and, on average, displays a more stable and higher water table than gullied areas within the footprint (Fig 4). It is therefore possible that the reason for our inability to model night-time respiration is that respiration in the gully systems and vegetated areas are subject to temporally divergent dynamics. Gatis et al. (2019) reported, using chamber-based measurements over two growing seasons in an eroded blanket bog peatland, that both photosynthetic CO_2 uptake and ecosystem respiration were lower in the eroded areas (peat pans) than in the vegetated areas (in their case, the hagged remnant areas of blanked bog surface). As the distribution of gullies within the footprint was relatively uniform amongst the prevalent wind directions, we were unable to partition the contribution of gullies versus vegetated areas akin to e.g., Pelletier et al. (2015). Gullies also act as short-term water bodies during periods of high precipitation, as well as a reservoir of snow for up to several weeks after snowmelt on the vegetated ground, so it is likely that there is a higher degree of insulation during such periods, whereas the ground heat flux during periods when the bare (black) surface is exposed is likely to be higher than on vegetated peat (e.g., Price et al., 1998). Future planned

improvements to the site through additional instrumentation in a representative gully close to the existing system will hopefully allow us to better explain the observed temperature responses in this ecosystem. Finally, peatland restoration work (gully reprofiling, ground smoothing, mowing for donor mulching material) was carried out during the monitoring period, although this did not extend into the footprint. It is possible that some minor interference from this work is occasionally included in our measurements, although we excluded any data where spectral responses clearly indicated loss of high-frequency data. There will be no further restoration activities in the 500 m radius surrounding the fetch and hence future data will shed further light on whether the difficulties in modelling the night-time temperatures were in relation to disturbances caused by nearby movement of soil.

The likely impacts of a 'do nothing' scenario as opposed to restoration of this and other eroded blanket peatlands in the global context of climatic change demands further consideration. Restoration of upland and mountain peatland locations carries a not inconsiderable cost due to the limited accessibility in space and time, however, current scenarios for the UK include both an increased frequency and severity of extreme rainfall events as well as summer droughts and potentially higher incidence of wildfires (UK Met Office, 2020). Widespread drying of European peatlands over the last 200 years, as a consequence of compound factors such as drainage or other management in combination with climatic changes, has been demonstrated by Swindles et al (2019) using testate amoeba records. Heavy rain events have been documented to lead to new peat erosion (e.g., Hulme and Blyth, 2017) and hence direct carbon losses, leaving the newly eroded peat surface exposed to other forces that could cause additional wind-blown and wind-driven rain erosion (Foulds and Warburton, 2007) and increased on-site gaseous emissions (Evans et al., 2006; Gallego-Sala and Prentice, 2013). Indeed, observations on this site suggested significant impact of the Storm Frank intense rainfall (29-30 December 2015) around the area of what is currently the flux tower footprint. There were also negative impacts on restoration work on a nearby location, where the rainfall washed out nearly all of a thin mulch of vegetation that had been laid onto bare peat areas in an initial restoration effort (Peatland Action data, S. Corcoran, Cairngorms National Park Authority, pers. Comm.). Using a peat erosion model (PESERA-PEAT) with seven different global climate models, Li et al. (2017) found that erosion rates for many Northern peatlands may increase by the 2080s. The pre-restoration state of our monitored eroded mountain blanket bog is that of a significant net CO_2 source to the atmosphere and annual carbon budgets that contained more of the 2018 drought period were nearly twice as high as budgets that included a period of more average climatic conditions. If our findings are representative of the wider state of eroded peatlands across the UK, such areas cover 4280 km^2 in the UK (Evans et al, 2017) and thus may presently be

462 considerable contributors to the UKs net CO_2 emissions from peatlands and the land use (LULUCF)
463 sector generally. This work therefore contributes to a growing body of evidence that current total
464 peatland emissions across Europe are largely characterised by the significant emissions from
465 degraded areas, which completely overrides any remaining sequestration potential from undamaged
466 peatland areas (Leifeld and Menichetti, 2018), and thereby strengthens calls for mitigation of their
467 carbon emissions. Future discussions and prioritisation of restoration activities, however, also need
468 to interrogate the carbon benefits of restoration of eroded upland peatlands against the significant
469 fossil fuel emission cost of restoration. At present, restoration of such eroded peatlands is still at
470 early stages, with few sites that have been rewetted more than a handful of years ago, and so the
471 carbon benefits of restoration can also not yet be assessed.

472

473 **Acknowledgements**

474 We are grateful to Balmoral Estate for access permissions and logistic aid with site instrumentation
475 and maintenance, Dr Ben Winterbourn for assistance in establishing the field site and Stephen
476 Corcoran at the Cairngorms National Park Authority for access to restoration site boundary data,
477 peat depth measurements, wider site observations and critical comments on an earlier version of
478 this manuscript.

479

480 **References**

481 Bechtold M, Schlaffer S, Toemeyer B, De Lannoy G (2018) Inferring Water Table Depth Dynamics
482 from ENVISAT-ASAR C-Band Backscatter over a Range of Peatlands from Deeply-Drained to Natural
483 Conditions. Rem Sensing 10(4), 536. https://doi.org/10.3390/rs10040536.

484 Birnie RV (1993) Erosion rates on bare peat surfaces in Shetland. Scottish Geographical Magazine
485 109(1):, 12–17, https://doi:10.1080/00369229318736871.

486 Bradshaw R, McGee E. (1988) The extent and time-course of mountain blanket peat erosion in
487 Ireland. New Phytologist 108: 219-224. https://doi.org/10.1111/j.1469-8137.1988.tb03699.x.

488 Beck H, Zimmermann N, McVicar T, Vergopolan N., Berg A, Wood EF (2018) Present and future
489 Köppen-Geiger climate classification maps at 1-km resolution. Scientific Data 5: 180214.
490 https://doi.org/10.1038/sdata.2018.214.

491 Carling PA, Glaister MS, Flintham TP (1997) The erodibility of upland soils and the design of
492 preafforestation drainage networks in the United Kingdom. Hydrological Processes, 11(15): 1963–

1980, https://ui.adsabs.harvard.edu/link_gateway/1997HyPr...11.1963C/doi:10.1002/(SICI)1099-1085(199712)11:15%3C1963::AID-HYP542%3E3.0.CO;2-M.

Carrara A, Kowalski AS, Neirynck J, Janssens IA, Yuste JC, Ceulemans R (2003) Net ecosystem CO_2 exchange of mixed forest in Belgium over 5 years. Agricultur Forest Meteorol 119(3–4): 209–227. https://doi.org/10.1016/S0168-1923(03)00120-5 .

Clay GD, Dixon S, Evans MG, Rowson JG, Worrall F (2011) Carbon dioxide fluxes and DOC concentrations of eroding blanket peat gullies. Earth Surface Processes and Landforms 37: 562-571. et al., 2011. https://doi.org/10.1002/esp.3193 .

Congedo L. (2016). Semi-Automatic Classification Plugin Documentation. DOI: http://dx.doi.org/10.13140/RG.2.2.29474.02242/1.

Dixon, S.D., Worrall, F., Rowson, J.G., Evans, M.G. (2015) Calluna vulgaris canopy height and blanket peat CO_2 flux: Implications for management. Ecological Engineering 75: 497-505. https://doi.org/10.1016/j.ecoleng.2014.11.047 .

Dixon SD, Qassim SM, Rowson JG et al (2014) Restoration effects on water table depths and CO_2 fluxes from climatically marginal blanket bog. Biogeochem 118: 159–176. https://doi.org/10.1007/s10533-013-9915-4.

Evans M, Lindsay J (2010) Impact of gully erosion on carbon sequestration in blanket peatlands. Clim Res 45: 31-41. https://doi.org/10.3354/cr00887 .

Evans M, Warburton J (2007) Geomorphology of Upland Peat: Erosion, Form and Landscape Change, Blackwell Publishing Ltd, Oxford.

Evans M, Warburton J, Yang J et al (2006). Eroding blanket peat catchments: Global and local implications of upland organic sediment budgets. Geomorphology 79: 45-57. https://doi.org/10.1016/j.geomorph.2005.09.015.

Evans C, Artz R, Moxley J, Smyth M-A, Taylor E, Archer N, Burden A, Williamson J, Donnelly D, Thomson A, Buys G, Malcolm H, Wilson D, Renou-Wilson F, Potts J (2017) Implementation of an emission inventory for UK peatlands. Report to the Department for Business, Energy and Industrial Strategy, Centre for Ecology and Hydrology, Bangor. 88pp. Available at https://naei.beis.gov.uk/reports/reports?report_id=980.

Evans CD, Peacock M, Baird AJ, Artz RRE, Burden A et al. (2021). Overriding water table control on managed peatland greenhouse gas emissions. Nature 593, 548–552. https://doi.org/10.1038/s41586-021-03523-1.

524 Falge E, Baldocchi D, Olson R et al (2001) Gap filling strategies for defensible annual sums of net
525 ecosystem exchange. Agric For Meteorol 107:43–69. https://doi.org/10.1016/S0168-1923(00)00225-
526 2.

527 Foulds SA, Warburton J (2007) Wind erosion of blanket peat during a short period of surface
528 desiccation (North Pennines, Northern England). Earth Surface Processes and Landforms 32: 481-
529 488. https://doi.org/10.1002/esp.1422.

530 Frolking SE, Bubier JL, Moore TR et al (1998) Relationship between ecosystem productivity and
531 photosynthetically active radiation for northern peatlands. Global Biogeochem Cycles 12: 115-126.
532 https://doi.org/10.1029/97GB03367.

533 Gallego-Sala AV, Prentice IC (2013) Blanket bog biome endangered by climate change. Nature
534 Climate Change 3: 152-155. https://doi.org/10.1038/nclimate1672.

535 Gatis N, Benaud P, Ashe J, Luscombe DJ, Grand-Clement E, Hartley IP, Anderson K, Brazier RE (2019)
536 Assessing the impact of peat erosion on growing season CO_2 fluxes by comparing erosional peat pans
537 and surrounding vegetated haggs. Wetlands Ecol Manag 27: 187-205.
538 https://doi.org/10.1007/s11273-019-09652-9.

539 Giorgi F, Raffaele F, Coppola E (2019) The response of precipitation characteristics to global warming
540 from climate projections. Earth Syst Dynam 10: 73–89, https://doi.org/10.5194/esd-10-73-2019 .

541 Hambley G, Andersen R, Levy P, Saunders M, Cowie N, Teh YA, Hill T (2019) Net ecosystem exchange
542 from two formerly afforested peatlands undergoing restoration in the Flow Country of northern
543 Scotland. Mires and Peat 23: 1-14. https://doi.org/10.19189/MaP.2018.DW.346.

544 Helfter C, Campbell C, Dinsmore KJ, Drewer J, Coyle M, Anderson M, Skiba U, Nemitz E, Billett MF,
545 Sutton MA (2015) Drivers of long-term variability in CO_2 net ecosystem exchange in a temperate
546 peatland. Biogeosciences 12: 1799–1811. https://doi.org/10.5194/bg-12-1799-2015.

547 Hulme PD, Blyth AW (2017) Observations on the erosion of blanket peat in Yell, Shetland.
548 Geografiska Annaler: Series A, Physical Geography 67: 1985.
549 https://doi.org/10.1080/04353676.1985.11880135.

550 IPCC (2018) Special Report: Global Warming of 1.5 ºC. https://www.ipcc.ch/sr15/

551 IPCC (2014) 2013 Supplement to the 2006 IPCC Guidelines for National Greenhouse Gas Inventories:
552 Wetlands, Hiraishi, T., Krug, T., Tanabe, K., Srivastava, N., Baasansuren,J., Fukuda, M. and Troxler,
553 T.G. (eds). Published: IPCC, Switzerland.

554 Järveoja J, Nilson MB, Crill PM, Peichl M (2020) Bimodal diel pattern in peatland ecosystem
555 respiration rebuts uniform temperature response. Nature Comms 11: 4255.
556 https://doi.org/10.1038/s41467-020-18027-1.

557 Juszczak R, Humphreys E, Acosta M et al (2013) Ecosystem respiration in a heterogeneous temperate
558 peatland and its sensitivity to peat temperature and water table depth. Plant Soil 366: 505–520.
559 https://doi.org/10.1007/s11104-012-1441-y.

560 Kljun N, Calanca P, Rotach MW, Schmid HP (2015) A simple two-dimensional parameterisation for
561 Flux Footprint Prediction (FFP). Geosci Model Dev 8: 3695-3713. https://doi.org/10.5194/gmd-8-
562 3695-2015.

563 Lafleur PM, Moore TR, Roulet NT, Frolking S (2005) Ecosystem respiration in a cool temperature bog
564 depends on peat temperature but not water table. Ecosystems 8: 619-629.
565 https://doi.org/10.1007/s10021-003-0131-2.

566 Lafleur PM, Roulet NT, Bubier JL, Frolking S, Moore TR (2003) Interannual variability in the peatland-
567 atmosphere carbon dioxide exchange at an ombrotrophic bog. Global Biogeochem Cycles 17: 1036,
568 https://doi.org/10.1029/2002GB001983.

569 Lee S-C, Christen A, Black AT, Johnson MS, Jassal RS, Ketler R, Nesic Z, Merkens M (2017) Annual
570 greenhouse gas budget for a bog ecosystem undergoing restoration by rewetting, Biogeosciences
571 14: 2799–2814, https://doi.org/10.5194/bg-14-2799-2017.

572 Lees KJ, Artz RRE, Chandler D, Aspinall T, Boulton CA, Buxton J, Cowie NR, Lenton TM (2021) Using
573 remote sensing to assess peatland resilience by estimating soil surface moisture and drought
574 recovery. Sci Total Environment 761: 143312. https://doi.org/10.1016/j.scitotenv.2020.143312.

575 Leifeld J, Menichetti L (2018) The underappreciated potential of peatlands in global climate change
576 mitigation strategies. Nature Comm 9: 1071. https://doi.org/10.1038/s41467-018-03406-6 .

577 Leifeld J, Wüst-Galley C, Page S (2019) Intact and managed peatland soils as a source and sink of
578 GHGs from 1850 to 2100. Nat Clim Change 9: 945–947. et al 2019. https://doi.org/10.1038/s41558-
579 019-0615-5.

580 Levy PE, Gray A (2015). Greenhouse gas balance of a semi-natural peatbog in northern Scotland.
581 Environment Res Letters 10: https://doi:10.1088/1748-9326/10/9/094019 .

582 Li-COR (2015) Li-7200 RS enclosed CO_2/H_2O analyser, Instruction Manual. Li-COR Biosciences,
583 Lincoln, Nebraska. Available at: https://licor.app.boxenterprise.net/s/k8b90wiwdhietarx04qd.

584 Li P, Holden J, Irvine B, Mu X et al., (2017) Erosion of Northern Hemisphere blanket peatlands under
585 21st- century climate change. Geophysical Research Letters 44: 3615-3623.
586 https://ui.adsabs.harvard.edu/link_gateway/2017GeoRL..44.3615L/doi:10.1002/2017GL072590..

587 Limpens J, Berendse F, Blodau C, Canadell JG, Freeman C, Holden J, Roulet N, Rydin H, Schaepman-
588 Strub G (2008) Peatlands and the carbon cycle: from local processes to global implications – a
589 synthesis. Biogeosciences 5: 1475 – 1491. https://doi.org/10.5194/bg-5-1475-2008 .

590 Lloyd J, Taylor JA (1994) On the temperature dependence of soil respiration. Functional Ecology 8:
591 315–323. https://doi.org/10.2307/2389824.

592 Loisel J, Gallego-Sala AV, Amesbury MJ et al. (2021) Expert assessment of future vulnerability of the
593 global peatland carbon sink. Nat. Clim. Chang. 11: 70–77. https://doi.org/10.1038/s41558-020-
594 00944-0.

595 McNamara NP, Plant T, Oakley S, Ward S, Wood C, Ostle N (2008) Gully hotspot contribution to
596 landscape methane (CH_4) and carbon dioxide (CO_2) fluxes in a northern peatland. Sci Total Environ
597 404: 354-360. https://doi.org/10.1016/j.scitotenv.2008.03.015

598 Lowe JA, Bernie D, Bett P, Bricheno L et al (2018) UKCP18 National Climate Projections. Met Office
599 Hadley Centre, Exeter. https://www.metoffice.gov.uk/research/approach/collaboration/ukcp/index

600 Nakai T, Shimoyama K (2012) Ultrasonic anemometer angle of attack errors under turbulent
601 conditions. Agr Forest Meterol 162-163: 14-26. http://dx.doi.org/10.1016/j.agrformet.2012.04.004.

602 Nugent KA, Strachan IB, Roulet NT, Strack M, Frolking S, Helbig M (2019) Prompt active restoration
603 of peatlands substantially reduces climate impact. Environ Res Lett 14: 12403.
604 https://doi.org/10.1088/1748-9326/ab56e6.

605 Pastukhov AV, Kaverin DA (2016) Ecological state of peat plateaus in northeastern European Russia.
606 Russian J Ecol 47: 125-132. https://link.springer.com/article/10.1134/S1067413616010100.

607 Paustian K, Lehmann J, Ogle S, Reay D, Robertson P, Smith P (2016) Climate-smart soils. Nature 532:
608 49-57. https://doi.org/10.1038/nature17174.

609 Pelletier L, Strachan IB, Roulet NT et al (2015) Effect of open water pools on ecosystem scale surface-
610 atmosphere carbon dioxide exchange in a boreal peatland. Biogeochem 124: 291–304.
611 https://doi.org/10.1007/s10533-015-0098-z.

612 Price J, Rochefort L, Quinty F (1998) Energy and moisture considerations on cutover peatlands:
613 surface microtopography, mulch cover and *Sphagnum* regeneration. Ecol Eng 10: 293-312.
614 https://doi.org/10.1016/S0925-8574(98)00046-9.

615 Renou-Wilson F, Moser G, Fallon D, Farrell CA, Müller C, Wilson D (2019) Rewetting degraded
616 peatlands for climate and biodiversity benefits: Results from two raised bogs. Ecol Eng 127: 547-560.
617 https://doi.org/10.1016/j.ecoleng.2018.02.014.

618 Rivington M, Spencer M (2020) Snow Cover and Climate Change on Cairngorm Mountain: A report
619 for the Cairngorms National Park Authority. The James Hutton Institute, Aberdeen, UK. Available at:
620 https://cairngorms.co.uk/wp-content/uploads/2020/07/Snow-cover-and-climate-change-on-
621 Cairngorm-Report-v3-3-6-20-with-appendix.pdf

622 Selkirk JM, Saffigna LR (2018) Wind and water erosion of a peat and sand area on subantarctic
623 Macquarie Island. Arctic, Antarctic Alpine Res 31: 1999.
624 https://doi.org/10.1080/15230430.1999.12003326.

625 Sottocornola M, Kiely G (2005) An Atlantic blanket bog is a modest CO_2 sink. Geophys Res Lett 32:
626 L23804, https://doi:10.1029/2005GL024731.

627 Sottocornola M, Kiely G (2010) Hydro-meteorological controls on the CO_2 exchange variation in an
628 Irish blanket bog, Agr Forest Meteorol 150: 287–297, https://doi:10.1016/j.agrformet.2009.11.013.

629 Strack M, Zuback YCA (2013) Annual carbon balance of a peatland 10 yr following restoration.
630 Biogeosciences 10: 2885–2896. https://doi.org/10.5194/bg-10-2885-2013.

631 Swindles GT, Morris PJ, Mullan DJ et al. (2019) Widespread drying of European peatlands in recent
632 centuries. Nat. Geosci. 12: 922–928. https://doi.org/10.1038/s41561-019-0462-z.

633 Tomlinson RW (2009) The erosion of peat in the uplands of Northern Ireland. Irish Geography 14:
634 1981. https://doi.org/10.1016/j.agrformet.2012.04.004 .

635 Waddington JM, Morris PJ, Kettridge N, Granath G, Thompson DK, Moore PA (2015) Hydrological
636 feedbacks in northern peatlands. Ecohydrology 8(1): pp.113-127. https://doi.org/10.1002/eco.1493.

637 Wilson D, Dixon SD, Artz RRE, Smith TEL, Evans CD, Owen HJF, Archer E, Renou-Wilson F (2015)
638 Derivation of greenhouse gas emission factors for peatlands managed for extraction in the Republic
639 of Ireland and the United Kingdom. Biogeosciences 12: 5291–5308. https://doi.org/10.5194/bg-12-
640 5291-2015.

641 Wilson D, Farrell CA, Fallon D, Moser M, Müller C, Renou-Wilson F (2016) Multiyear greenhouse gas
642 balances at a rewetted temperate peatland. Global Change Biol 22: 4080-4095.
643 https://doi.org/10.1111/gcb.13325 .

644 Wilson P, Clark R, McAdam JH, Cooper EA (1993). Soil erosion in the Falkland Islands: an assessment.
645 Appl Geography 13: 329-352. https://doi.org/10.1016/0143-6228(93)90036.

646 Worrall F, Rowson JG, Evans MG, Pawson R, Daniels S, Bonn A (2011) Carbon fluxes from eroding
647 peatlands – the carbon benefit of revegetation following wildfire. Earth Surface Proc Landforms 36:
648 01487-1498. https://doi.org/10.1002/esp.2174.

649 Yu ZC (2012) Northern peatland carbon stocks and dynamics: a review. Biogeosciences 9: 4071–4085.
650 https://doi.org/10.5194/bg-9-4071-2012 .

651 Yunker MB, Macdonald RW, Fowler BR, Cretney WJ, Dallimore SR, McLaughlin FA et al (1991)
652 Geochimica et Cosmochimica Acta 55: 255-273. https://doi.org/10.1016/0016-7037(91)90416-3 .

Table 1. Monthly light use response parameters for periods with data availability during the monitoring period. NA = Insufficient data for month.

	alpha			A_{max}			Rm			r2		
month	**2018**	**2019**	**2020**	**2018**	**2019**	**2020**	**2018**	**2019**	**2020**	**2018**	**2019**	**2020**
May	NA	0.01	NA	NA	1.61	NA	NA	0.44	NA	NA	0.28	NA
Jun	NA	0.01	NA	NA	2.26	NA	NA	0.34	NA	NA	0.22	NA
Jul	0.04	0.02	NA	7.48	6.18	NA	2.42	1.19	NA	0.94	0.52	NA
Aug	0.04	0.02	0.04	8.76	7.74	9.54	1.99	1.09	1.87	0.83	0.58	0.81
Sep	0.03	0.02	0.04	7.50	7.47	6.59	2.15	1.21	1.58	0.59	0.62	0.74
Oct	0.04	0.02	0.03	3.11	3.57	5.16	1.91	0.92	1.24	0.2	0.34	0.6

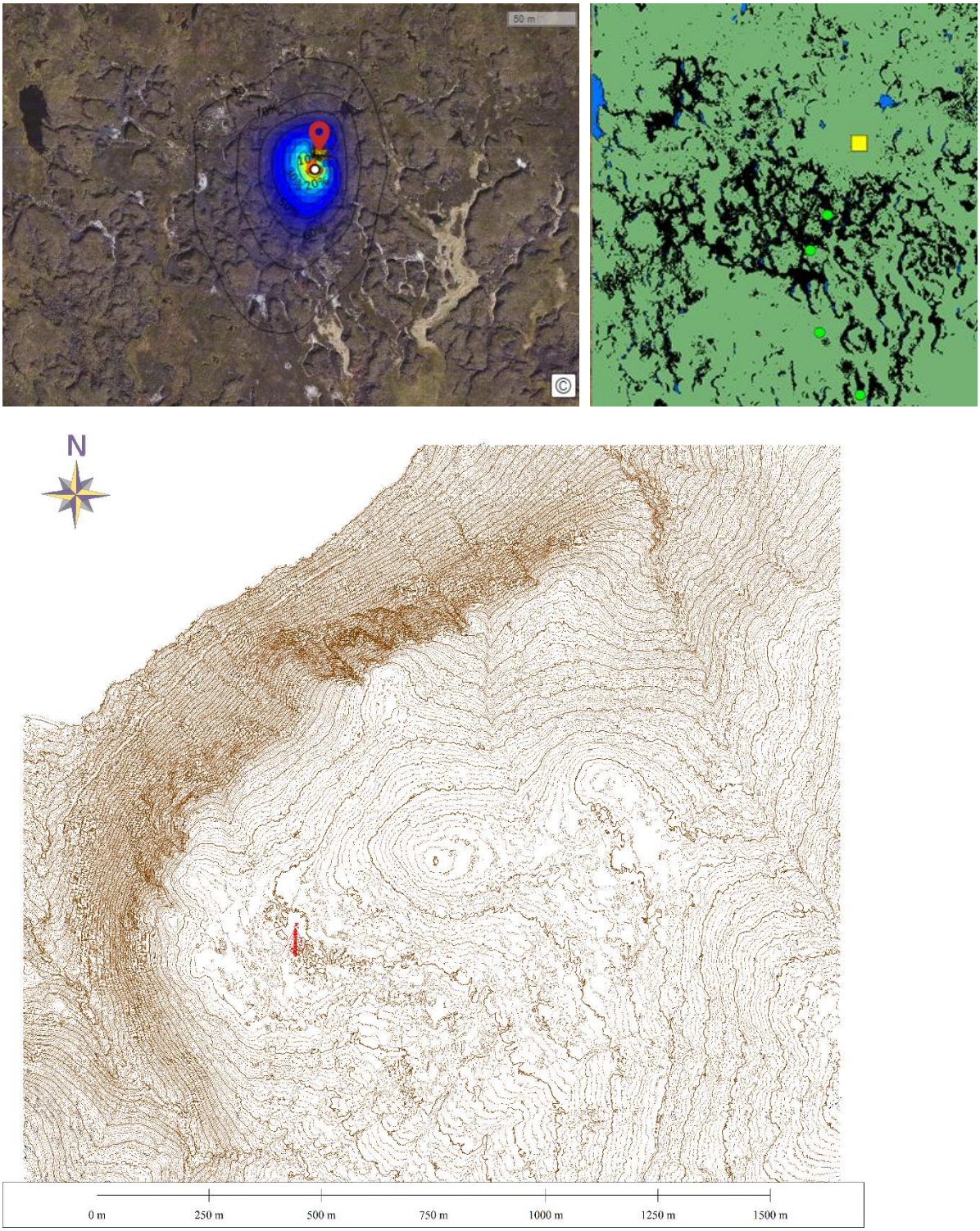

Fig. 1. Top Left: Footprint across the eroded area as estimated using Kljun et al. 2015 within Tovi for the 2018 data series. Tower location is at the marker. Footprint contours are shown in 10% intervals from 10-90% with a heatmap indicating up to the 50% interval. Top Right: Classification product in the footprint area, showing vegetated peat in green, water bodies in blue, and bare peat in gullies in black. The flux tower location is shown with a yellow square and ground validation in the vicinity of the tower are shown as green circles (this is an excerpt from a wider classified scene, hence only a small proportion of the ground validation points have been shown). Lower: Wider 2 km^2 area, with 1 m contours (LiDAR derived, thicker contours are 5 m intervals), tower location as marked.

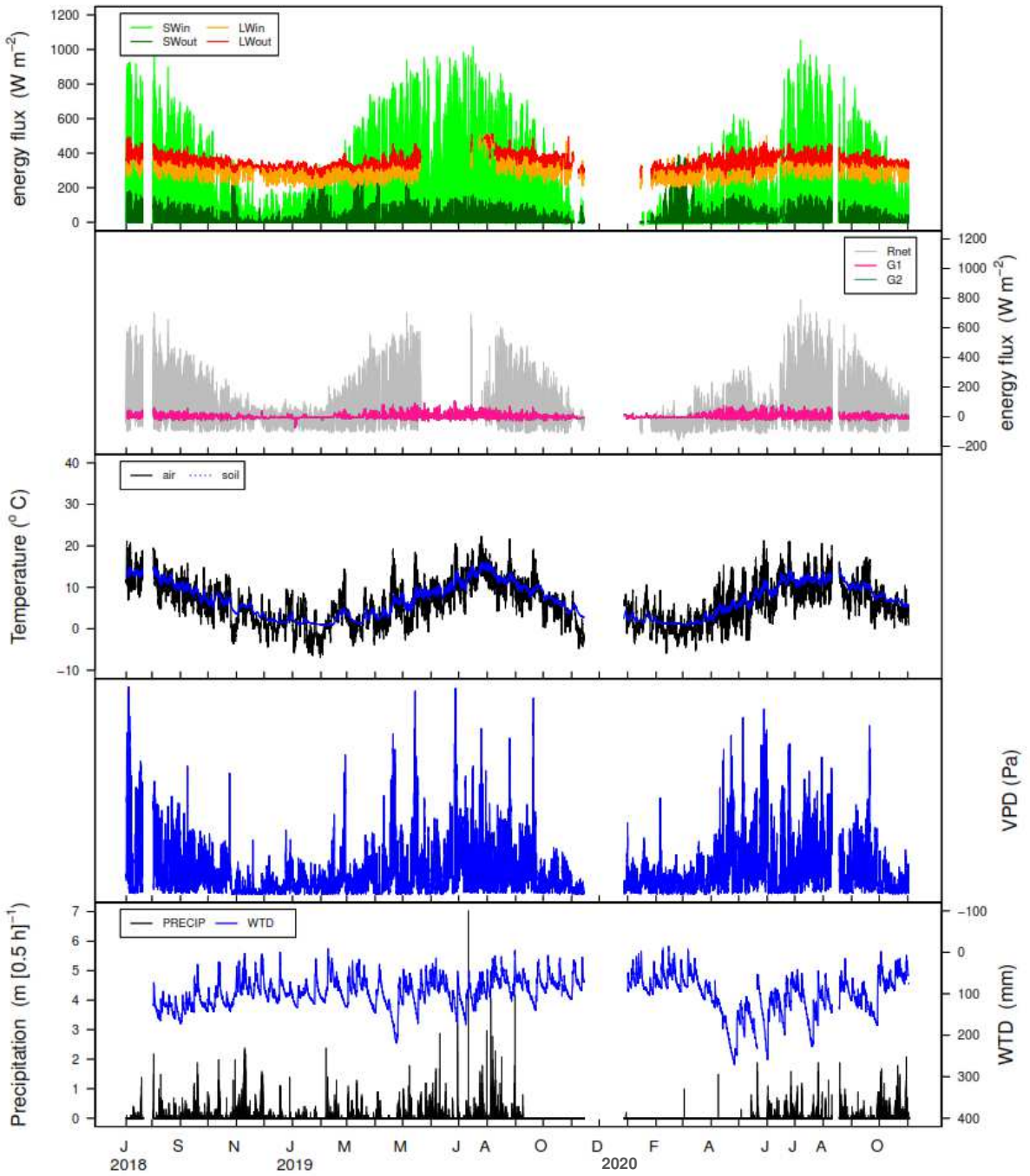

665 **Fig. 2.** Environmental variables monitored across the full monitoring period from July 2018 to
666 November 2020. In order, from top to bottom: Short- and long-wave incoming and outgoing energy
667 flux components: soil heat flux relative to net radiation; air and soil temperature vapour pressure
668 deficit and precipitation/water table depth. The longwave incoming and outgoing radiation data are
669 incomplete due to a faulty sensor; data for such periods have been omitted. Similarly, data for the
670 autumn of 2019 to early summer 2020 for precipitation are suspect due to a wire that was partially
671 damaged by rodents.

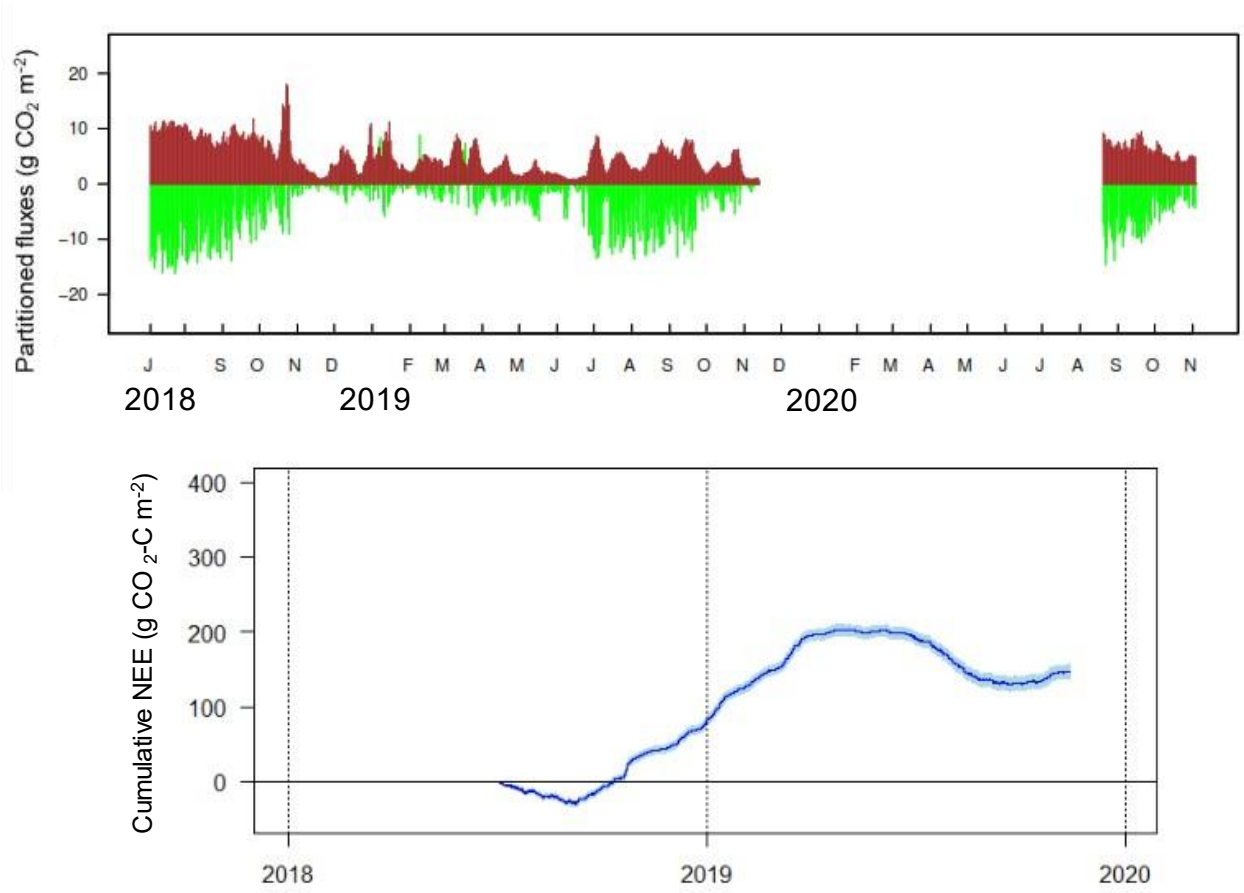

672

673 **Fig. 3.** Partitioning of GPP and Reco, based on the standard night-time respiration approach (upper)
674 for the entire monitoring period excluding the period where the CO_2/H_2O analyser was partially
675 blocked, and cumulative NEE (lower), starting at the beginning of the monitoring period (4 July 2018)
676 and ending on the last currently available monitoring date without significant data gaps of 14
677 November 2019).

678

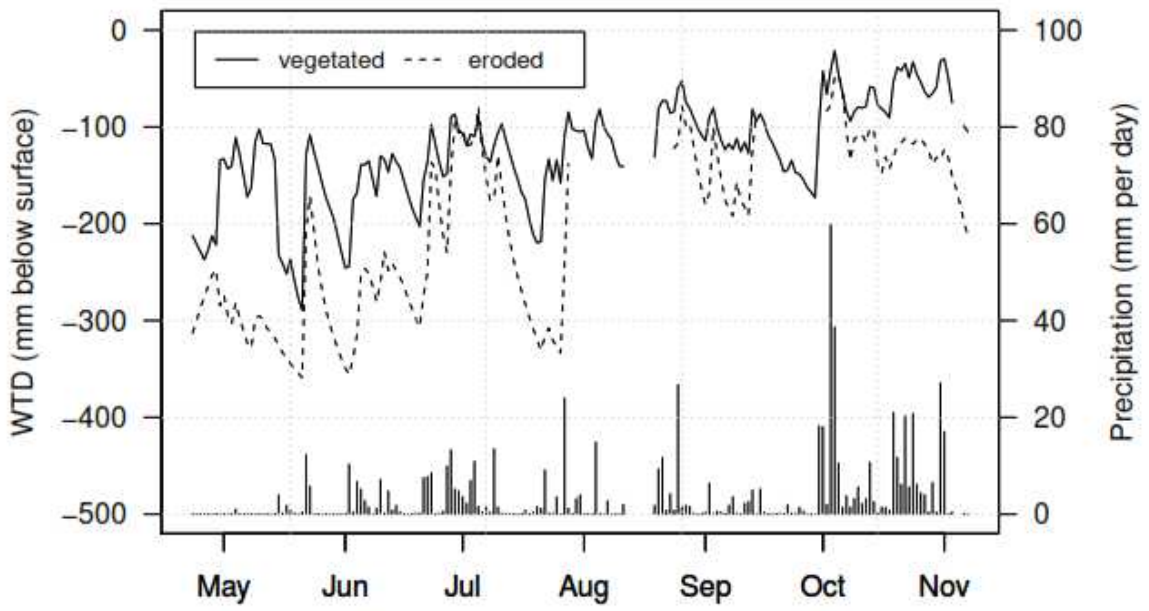

Fig. 4. Differences in water table depth dynamics between the water table dynamics measured directly adjacent to the flux tower (black line) against the water table dynamics adjacent to erosion gullies lower, stippled line), shown relative to precipitation events (black bars) during 2020. Observations shown are means of n=3 (flux tower and wider vegetated area) and n=4-6 (adjacent to erosion gullies) water level loggers.

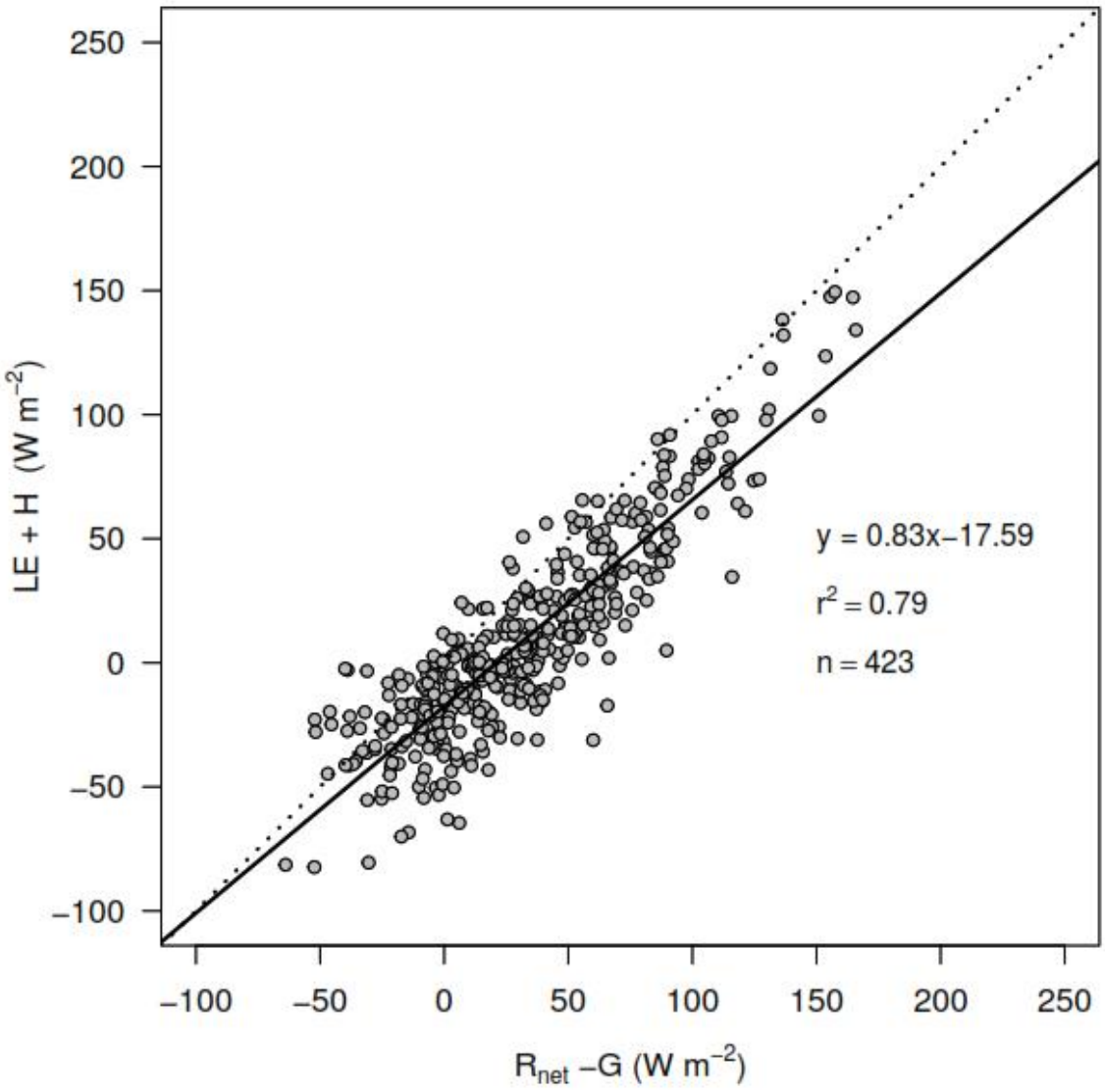

686

687 **SI Fig. 1.** Energy balance closure at the eroded peatland location, using daily sums to include storage
688 terms. The regression equation, determination coefficient (r^2), and number of data points (n) are
689 shown. Data include all 30-minute flux observations that have passed quality control for 30-min
690 periods when all energy balance terms were available. The solid black line shows the linear
691 regression. The dashed line shows the 1:1 linear relationship. The EBC based on half-hourly data was
692 y = 0.64 x -11.8, r^2 = 0.71, using 22807 observations (not shown).

693

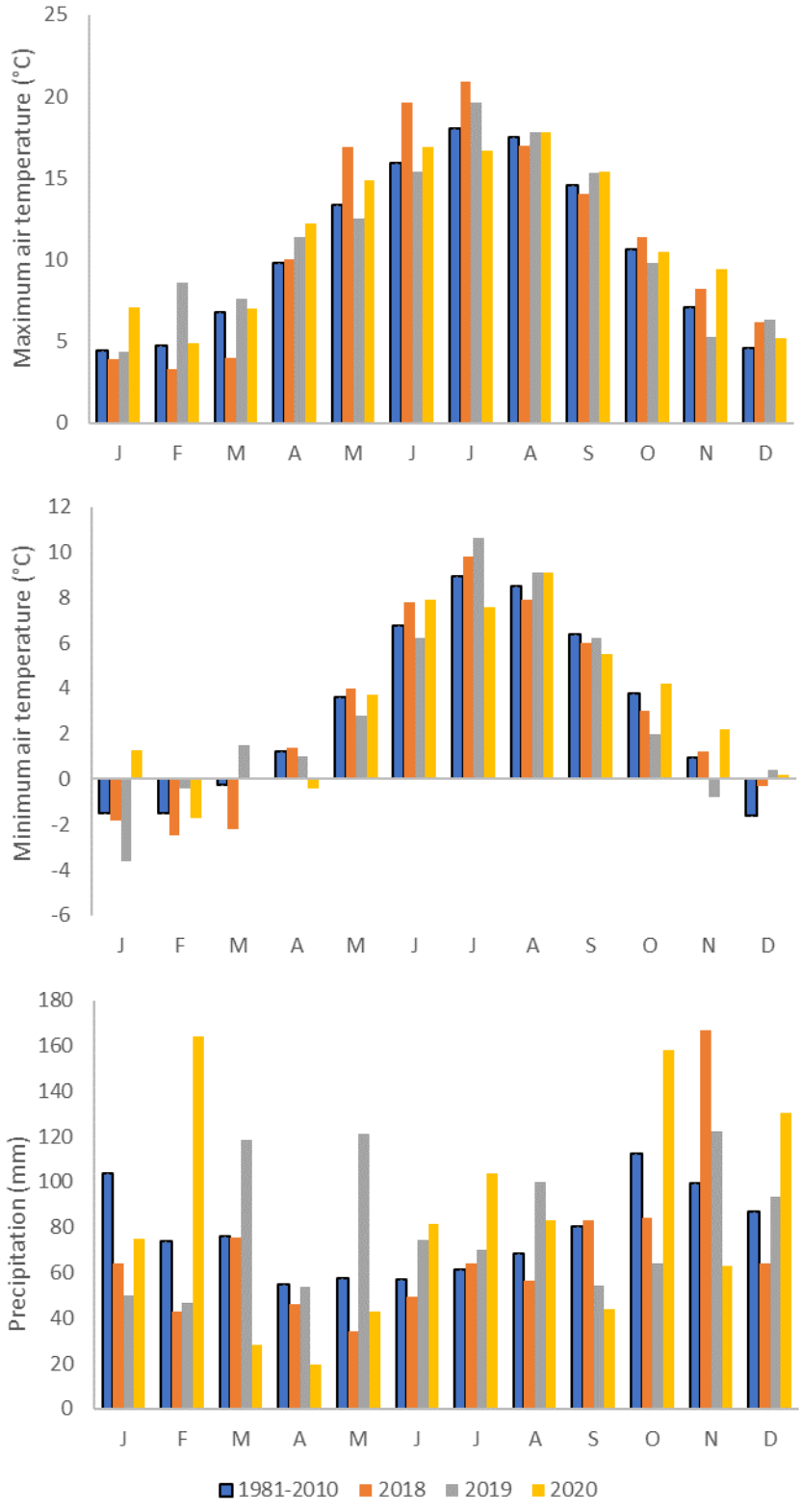

694

695 **SI Fig. 2.** Monthly average of daily maximum (upper), and minimum (middle) air temperature as well
696 as monthly sum of precipitation (lower) at the nearby Braemar weather station, for the observation
697 years compared with the 1981-2010 average.

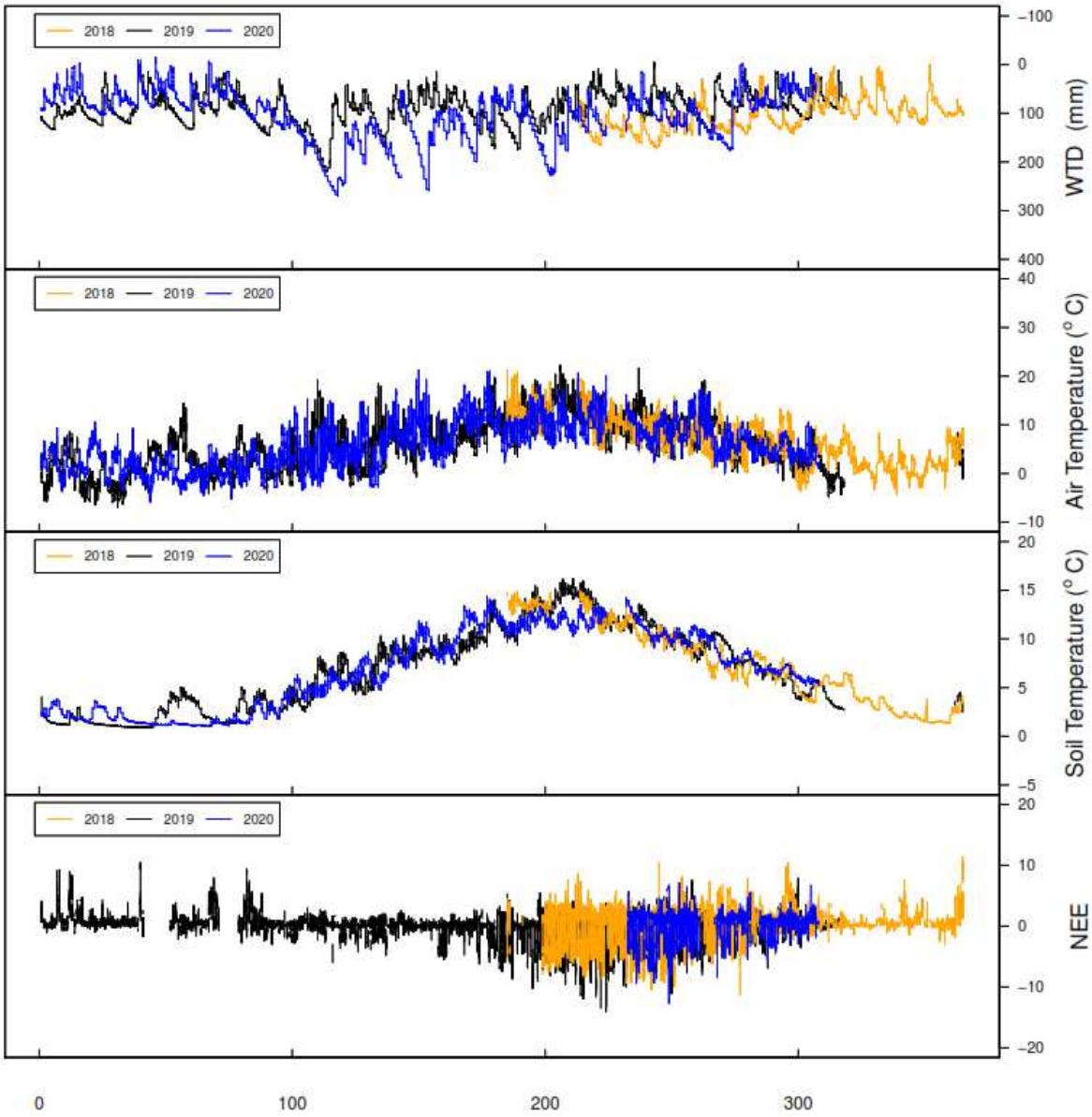

698

699 **SI Fig. 3.** Year-on-year comparison of measured WTD, air and soil temperature, and NEE, at Balmoral.

700 X axis depicts Day of Year.

701